Surface modified Acacia Senegal Gum based spherical hydrogel; fabrication, characterization, and kinetically optimized waste water treatment with remarkable adsorption efficiency

Rasha M.K. Mohamed

Department of Chemistry, College of Science, Jouf University, P.O. Box: 2014, Sakaka, Saudi Arabia
Department of Chemistry, Faculty of Science, Assiut University, P.O. Box: 71515, Assiut, Egypt

A B S T R A C T

Acacia Senegal Gum hydrogel (HASG) with swollen dimension less than 50 μm were fabricated, and chemically modified with versatile diethylenetriamine (D-amine) to tailor the surface properties for environmental remediation.

Negatively charged metal ions, for example, chromate (Cr(III)), dichromate (Cr(VI)), and arsenate (As(V)) were removed from aqueous media by using modified hydrogels (m-HASG). The FT-IR spectra revealed some new peaks due to D-amine treatment. The zeta potential measurements confirm a positively charged surface of HASG upon D-amine modification at ambient conditions. The absorption studies revealed that 0.05 g feed of m-(HASG) possesses 69.8, 99.3, and 40.00% cleaning potential against As(V), Cr(VI), and Cr(III), respectively with 2 h contact time in deionized water. Almost comparable adsorption efficiency was achieved by the prepared hydrogels towards the targeted analytes dissolved in real water samples. Adsorption isotherms, for example, Langmuir, Freundlich and modified Freundlich isotherms were applied to the collected data. Briefly, Modified Freundlich isotherm manifested comparatively agreeable line for the all adsorbents pollutants with highest R^2 figure.

In addition, maximum adsorption capacity (Qm) with 217, 256, and 271 mg g^{-1} numerical values were obtained against As(V), Cr(VI), and Cr(III), respectively. In real water samples, 217, 256, and 271 mg g^{-1} adsorption capacity was represented by m-(HASG).

In brief, m-(HASG) is a brilliant material for environmental application as cleaner candidate towards toxic metal ions.

1. Introduction

The tremendous advancement and improvement in technology has brought industrialization and globalization that caused revolution in each field of life [1–3]. The massive industrialization has caused environmental degradation and as a result, many harmful pollutants are entering in various spheres of life [4]. Upon arrival into food chain through waste or drinking water, majority of the pollutants are up taken by body through breathing or skin absorption [5]. Majority of the health related issues are originated due to the induction of heavy metals into the environment, as investigated by various environmental scientists [6]. Accumulation of high heavy metal concentration is not related to direct impact of majority of pollutants; however, the gradual accumulation in the body causes

lethal effect [7]. In spite of these critical concerns, human exposure to the deadly pollutants in particular, in developing countries has been increasing due above said uncontrolled exercises [8]. Recent studies demonstrate that almost 600 million people around the world every year are exposed to threatening heavy metals [9].

Due to serious biological concerns, environment focusing researchers have been warning from the consequences of heavy metals and toxic dyes contamination [10,11]. Highly toxic Cr(VI) is found as an active candidate in the loss and alteration of various biological assays in living entities [12], whereas As(V) causes the uncoupling of oxidative phosphorylation of ATP, and may replace the similar phosphate groups [13–15]. Further contamination must be prevented to avoid the deadly consequences of the issues associated with heavy metals based effluents.

To coupe with the above, different techniques for example, membrane separation, chemical precipitation, electroflotation, reverse osmosis, and oxidation/reduction reaction processes have been used to treat heavy metals [16]. However, several shortcomings, for example, self-poisonous effect, durability of the methods, and most importantly, the high capital cost associated with the above cited methods hinder their applicabilities universally [17].

It is therefore proposed to design low cost methods based on rapid and environmentally sound technique originated from naturally abundant materials for hazardous species removal from aqueous systems.

This manuscript enlists a cost-effective technique for Acacia Senegal polymer chains crosslinking via DS crosslinking, and hereafter surface modification for adsorptive removal of toxic heavy metal from water widely used Acacia Senegal due to its positive role in hepatic failure, wattle blossom structure, efficient encapsulating and emulsifying agent, has attracted great attentions of many research groups [18,19]. Crosslinking of Acacia Senegal provides micro-matrix with potentially stable texture, and enhanced surface area that readily enables its chemical modification with various agents to generate additional functional groups [20]. Interestingly, biomaterials functionalized via various amines are studied to achieve environmental sustainability goals owing to amines quartering and complexing nature [21–23]. Thus, D-amine modified swellable Acacia Senegal matrix could effectively work in poisonous metal ions reduction. In brief, the crosslinking of Acacia Senegal chains via the doubly bonded terminal carbons of DS with alcoholic groups of Acacia Senegal was accomplished. The chemistry of DS is found hierarchical in protein and carbohydrate residue conjugation in single step [24]. D-amine utilization is aimed to achieve partial amination goals inline with the hazardous heavy metals adsorption [25]. The selection of biologically sound polymer, non-toxic texture, cost-effectiveness, and high yields of HASG, as well as, m-(HASG), in addition with fast removal of heavy metals was focused in the current investigation. In addition, the accomplished real water adsorption tests on the promising natural polymers is the targeted objective so that to check the applicability of the prepared hydrogel for practical environmental remediation purpose.

2. Materials and method

2.1. Materials

Acacia Senegal (branched polymeric gum, Mw: 2500,000 g mol^{-1}, Sigma Aldrich), divinyl sulfone (crosslinker, DS, 98%, Sigma Aldrich), sodium bis (2-ethylhexyl) sulfosuccinate (Surfactant, AOT, 98%, Sigma-Aldrich), Diethylenetriamine (Modifying, D-Amine, 98%, Sigma-Aldrich), and epichlorohydrin (Madiator modifying agent, ECH, 98%, Sigma-Aldrich) were used as main ingredients for hydrogel fabrication. Gasoline (Total, 95 octanes) was obtained from local vendor whereas, acetone (99%, Birkim) was obtained from Sigma Aldrich. All Fresh aqueous solutions were prepared in pure distilled water (DI) 18.2 MΩ cm (Millipore-Direct Q UV3).

Similarly, ultra-pure distilled water 18.2 MΩ cm (Millipore-Direct Q UV3) was used to prepare metal salt solutions with highest purity.

2.2. Synthesis of HASG

Acacia Senegal based hydrogel (HASG) were prepared via commonly used reverse micellization method of AOT. Briefly, 1 g of Acacia Senegal powder were dispersed in 10 mL of 0.5 M NaOH solution, and stirred till complete dissolution. After 30 min, the prepared solution was added dropwise to 0.3 L AOT solution (0.1 M, in gasoline) under continuous mixing (1500 rpm) at room temperature. After 15 min, 0.24 mL DVS (1:1 mol ratio of polymer to crosslinker) was added into the stirring mixture, and the reaction was continued for 30 min to obtained crosslinked HASG. The prepared HASG were precipitated in 0.3 L acetone. The supernatant was decanted and the precipitated HASG were washed (ethanol-water 50:50, two times) to remove the unreacted compounds and ions. Finally, the HASG were dried (60 °C, oven) and further used.

2.3. Synthesis of m-(HASG)

The chemical modification of the prepared HASG was carried out by following an illustration in the literature with some modification (Anirudhan and Rauf, 2013). Initially, 1 g of HASG transferred to 20 mL NaOH solution (0.2 M) for 20 min, and washed with water through sufficient centrifugation. The swollen HASG were the mixed with 20 mL DMF, and immediately 4 mL of ECH was added to the stirring medium mixed for 60 min at 90 °C under 800 rpm stirring rate. After 1 h mixing, 5 mL D-amine (modifying agent) was added and mixed for 1 h at 800 rmp, and 90 °C. These modified material was completely precipitated in, and the supernatant was decanted. Then, the m-(HASG) were washed via the equal volume mixture of ethanol. The functionalized material was dried (50 °C, oven), and further used.

2.4. Characterization of HASG and m-(HASG)

Scanning Electron Microscope (SEM, Jeol JSM-5600 LV, 20 kV operating voltage) was used for visualization of HASG particles size. Before imaging, dried particles were put on a carbon tape on the stub, and then coated with a few nm thickness of gold under vacuum.

The functional groups of the materials were analyzed using Fourier Transform Infrared Spectroscopy (FT-IR, Perkin-Elmer) via ATR technique at 4 cm^{-1} resolution in range 4000–650 cm^{-1} spectral range.

Zeta potential measurements of HASG, and m-(HASG) suspended in DI water was recorded by using Zeta-Pals Zeta Potential Analyzer BIC (Brookhaven Inst. Corp.) The surface charge of HASG and m-(HASG) were thoroughly measured via dynamic light scattering (DLS) Brookhaven Ins. and Cor. 90 plus particle size analyzer instrument. The HASG and m-(HASG) were dispersed into DI water and filtered with a 5 μm of syringe filter before the measurements. Real water samples of Nestle pure drinking water were obtained from local grocery super store in Saudi Arabia.

2.5. Absorption experiments

Environmental remediation of m-(HASG) was examined by using arsenate, chromate, and dichromate solutions in water as adsorbate at room temperature. In this method, 0.05 g of m-(HASG) was mixed with 100 mL pollutants solution (250 mg mL^{-1}) in a
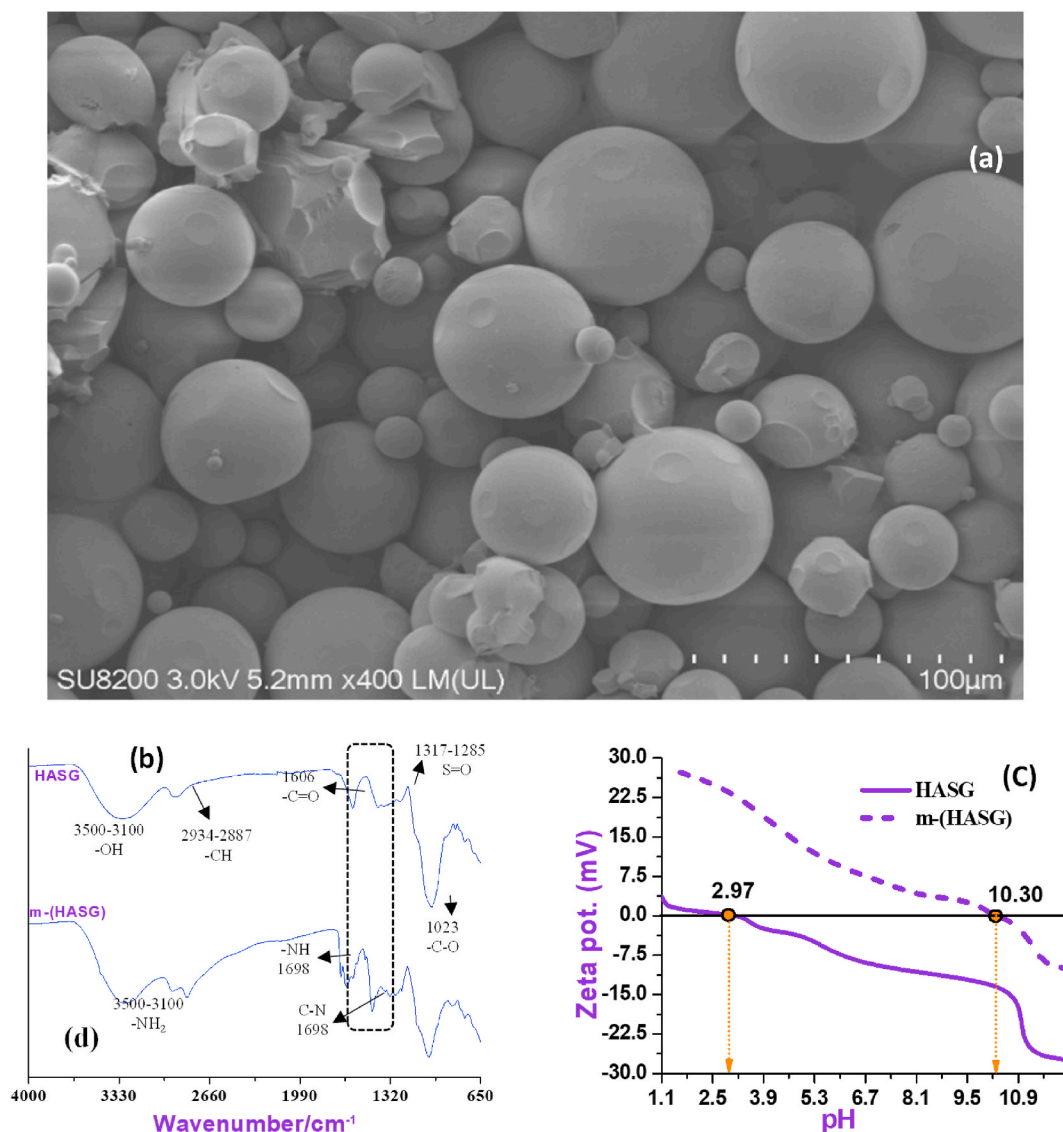

Fig. 1. (a) SEM images of the prepared HASG. (b) Comparisons of FT-IR spectra of HASG and m-(HASG), and (c) isoelectronic point (IEP) of HASG, and m-(HASG) by zeta potential measurements.

beaker, and stirred. Then, at various time intervals, 0.5 mL of sample was shifted from the stirring solution and subjected to AAS (Thermo Scientific, ICE 3000 series) analysis for concentration change.

Well recognized Nestle water was used as solvent and adsorption experiments were conducted to investigate the real water analysis against the targeted analytes. Similar procedure as mentioned above was used, and kinetic treatment was conducted.

3. Results and discussion

3.1. Synthesis of HASG and m-(HASG)

The crosslinked polymers with distinctive textures could be employed to different fields such as, adsorption of oppositely charged species, reduction of metal ions, and surface modification with suitable compounds [26,27]. A facile single-pot technique was used to prepare crosslinked HASG within AOT-Gasoline microemulsion system using DS as crosslinker. It is assumed that NaOH pre-treated biopolymers reside inside the reverse micelle core due to ionic interaction with the head group of AOT [28]. Upon addition of DS, the system energy is assumed to increase, and there become two possibilities to minimize the system energy, either the crosslinker molecules get inside the pre-loaded (with polymers) micelle cores or encapsulate in hollow micelle cores [29]. These reverse micelles further allow the crosslinking of polymer by species exchange during successive inter-micellar collisions, carried out through Brownian motion and/or mechanical mixing [30].

The possible crosslinking of Acacia Senegal Gum chains follow Michael type inter chains addition reaction of DS to the alcoholic group on saccharide units [31,32]. It is noteworthy to remark that slower exchange rate of species during successful collision control the size and shape of the prepared hydrogels due to the availability of fewer number of polymer units within spherical micelle cores for successive crosslinking. Fig. 1a give SEM image of HASG that gives the evidence of successful HASG synthesis in 5–30 μm size range. Prepared HASG were subjected to surface modification with ᴅ-amine for NH₂ functional groups generation. For this purpose, the dried HASG particles were treated with NaOH solution prior to modification for sequential ionization of OH groups on the hydrogels. The activated hydrogels were thereafter mixed with ECH for its possible reaction with epoxy ring using DMF as solvent at 90 °C. The appearance of pale yellowish color during the 1 h mixing of 5 mL ᴅ-amine with the stirring mixture indicate the fabrication of m-(HASG).

For successful crosslinking verification via DS, and thereafter modification with ᴅ-amine, the predictable functional groups of HASG based hydrogels were determined by using FT-IR spectroscopy. As illustrated in Fig. 1b, the specific peaks at 3100–3500, 2934–2888,1600, 1400, and 1033 cm⁻¹ were assigned to –OH, –CH, –C═O, and –C–O based functional groups on HASG, correspondingly. Further, the lower frequency peaks at around 1317 and 1285 cm⁻¹ were attributed to S═O groups of DS. The new peaks for the modified forms of HASG were obtained at 3300, 1698, 1654 and 1453 cm⁻¹ stretching vibrations which comes from –NH and C–N groups of ᴅ-amine thereby indicate the successful modification of the starting material. Owing to facile protonating and complexing nature, amines functionalized porous materials can be readily used for environmental and tremendous catalytic applications. Herein, the amine functionalized materials were readily used for adsorption in removing some toxic heavy metals such as arsenate, chromate, and dichromate. It was observed that the modified particles show enhanced adsorption capability in the proposed environmental remediation.

Overall surface charge provides important information about the material of interest for further use in various areas such a catalysis, biomedical and environmental applications. For this purpose, HASG and m-(HASG) were dispersed in DI water and kept till sufficient swelling in DI, and then filtrated through 5 μM pore size syringe filter for zeta potential measurements at varying pH, followed by DLS measurements. As can be seen in Fig. 1c, HASG give a negatively charged surface at neutral, as well as, highly basic conditions. However, m-(HASG) represent a positively charged surface both at neutral and acidic condition confirming the activity of positively charged multiple amines on m-(HASG) in the aqueous medium [33]. The isoelectric point (IEP) for HASG was observed at pH
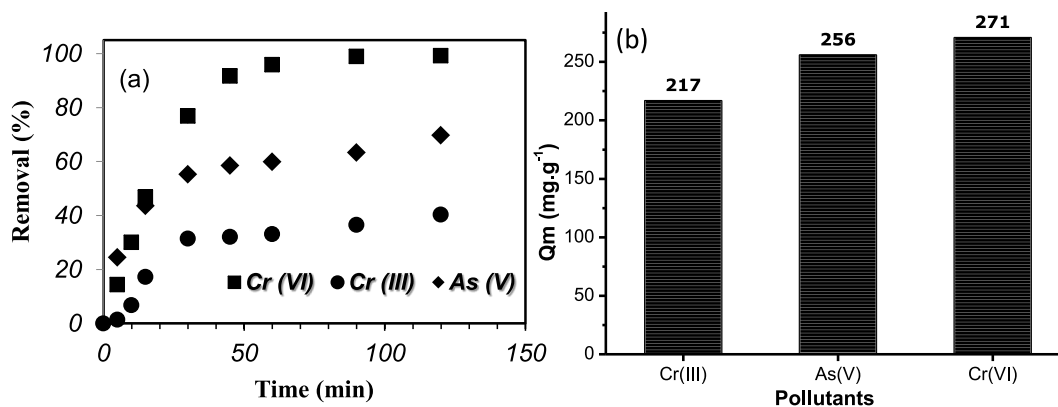

Fig. 2. Percent adsorption versus time (min) profile of (a) Cr(VI), As(V), and Cr(III) from respective salt solution (250 mg/mL⁻¹) and (b) Capability of the maximum adsorption amounts (mg.g⁻¹) of m-(HASG) towards various pollutants from the aqueous medium.

2.97, whereas, for m-(HASG) the neutral surface charge was achieved at pH 10.3.

3.2. Kinetic treatment of pollutants removal via m-(HASG)

In view of possessing positive charge, m-(HASG) were presumed as adsorbent for the removal of various heavy metals from water. The As (V), Cr (III), and Cr (VI)% removal via 0.05 g m-(HASG) in total 2 h contact time as shown in Fig. 2a was determined by applying a well-known mass balance equation given below:

$$Qt = (C_o–C_e)V/W \tag{1}$$

In this equation, Q_t represents the heavy metal amount adsorbed on 1 g of m-(HASG). The C_o and C_e give the heavy metal concentration at time 0 and equilibrium conc. Respectively. V is the volume (L) of the heavy metal solution, and W represents the weight (g) of m-(HASG).

Fig. 2a give a brief overview of kinetic terms calculated from adsorption on m-(HASG) feed in DI water. Interestingly, similar removal efficiency was represented by the administrated hydrogels in all adsorption experiments carried out in real water samples with similar experimental conditions (Supplementary Fig. S2a). As can be seen from the plotted points, around 99.3%, 69.8%, and 40.0% Cr (VI), As(V), and Cr(III) was removed from the respective adsorption batches via 0.05 g feed during 12 min mixing time.

Further, Supp. Fig. S1 show the effect of varying m-(HASG) amount (0.01, 0.025, 0.05, 0.10 and 0.15 g) on pollutants (250 mg mL^{-1} each) adsorption. Briefly, 100%, 99%, and 97% against Cr(VI), As(V), and Cr(III), respectively. However, up to 99.0%, 92.10% and 95.0% adsorption capacity was represented by 0.15 g feed (highest feed amount) from their aqueous salt solution in the total mixing time of 2 h (Supp. Fig. S1).

Fig. 2b demonstrates the max. adsorption (Q_m) obtained from Langmuir equation plot of variable initial on optimized m-(HASG) feed. As demonstrated in Fig. 2b, 271 mg/g Q_m was obtained from Cr (VI) based mixing batch. In addition, As(V), and Cr(III) represented 256 mg/g and 217 mg/g Q_m, respectively. In the meantime, 217, 254 and 266 mg/g adsoption capacity was represented by the prepared hydrogel in real water samples at same experimental conditions.

The proposed adsorption phenomena could be may be due to of chelation interaction of m-(HASG) D-amine with the heavy metals based pollutants previous assessments suggests a second order rate kinetics [34] for adsorption on porous surfaces.

Thus, the obtained adsorption data was checked for fitting in second order rate equation, which is given as follows;

Therefore, second order rate equation (2) was varified through the collected data:

$$t/Q_T = 1/K_2Q_E^2 + t/Q_E \tag{2}$$

In the above equation (2), K_2 represents second order rate constant, Q_t and Q_E are the amount of targeted contaminants adsorbed, and t is the total time taken at equilibrium.

Fig. 3a show the linear expression of equation (2) whereas, the quantitative varification is given in Table 1. The highest R^2 was obtained against Cr (III).

3.2.1. Kinetic optimization of pollutants adsorption on m-(HASG)

Three well-known adsorption isotherms for examples Langmuir, Fruendlich, and modified Fruendlich isotherms as given below were verified by plotting adsorption data points;

$$C_E/Q_E = 1/Q_MC_E + 1/Q_M.K_L \tag{3}$$

$$\ln(Q_E) = \ln(K_F) + 1/n_f.\ln (C_E) \tag{4}$$

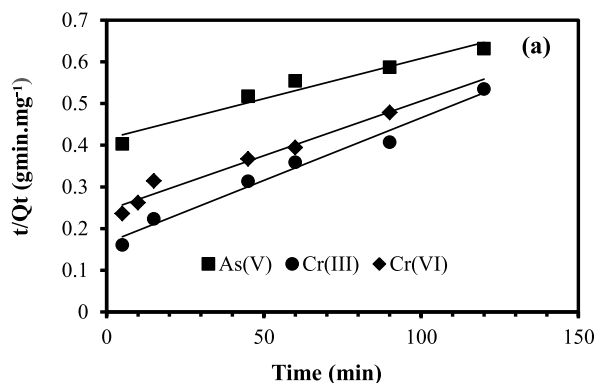$$\ln(Q_E/C_E) = \ln K_{mf} +(1/n_{mf} −1) \ln Q_E \tag{5}$$

Fig. 3. (a)Second order rate equation plot constructed from the data points obtained from adsorption on m-(HASG).

Table 1

Brief overview of the kinetic parameter calculated from the second order rate equation data obtained against DI water and real water (RW) sample adsorption experiments.

Parameter	Contaminants					
	Arsenic(V)		Chromium (III)		Chromium (VI)	
R^2	DI	RW	DI	RW	DI	RW
	0.96	0.96	0.98	0.98	0.97	0.97
K_2 (min.mg/g)	2.4×10^{-5}	2.3×10^{-5}	2.5×10^{-5}	2.5×10^{-5}	2.1×10^{-5}	2.7×10^{-5}

In mathematical expressions as mentioned above, equation (3) represents differentiated langmuir model where, C_E represents pollutant concentration at equilibrium, Q_E is the final pollutant amount adsorbed, Qm gives the max. adsorption capability of m-(HASG), and K_L is the equilibrium constant associated with Langmuir adsorption [35].

Langmuir model was varified for pollutants adsorption (Fig. 4a). As can be seen from the linear pattern of plots in Fig. 4a, the adsorption on m-(HASG) varifies the agreeable fit with high R^2 value.
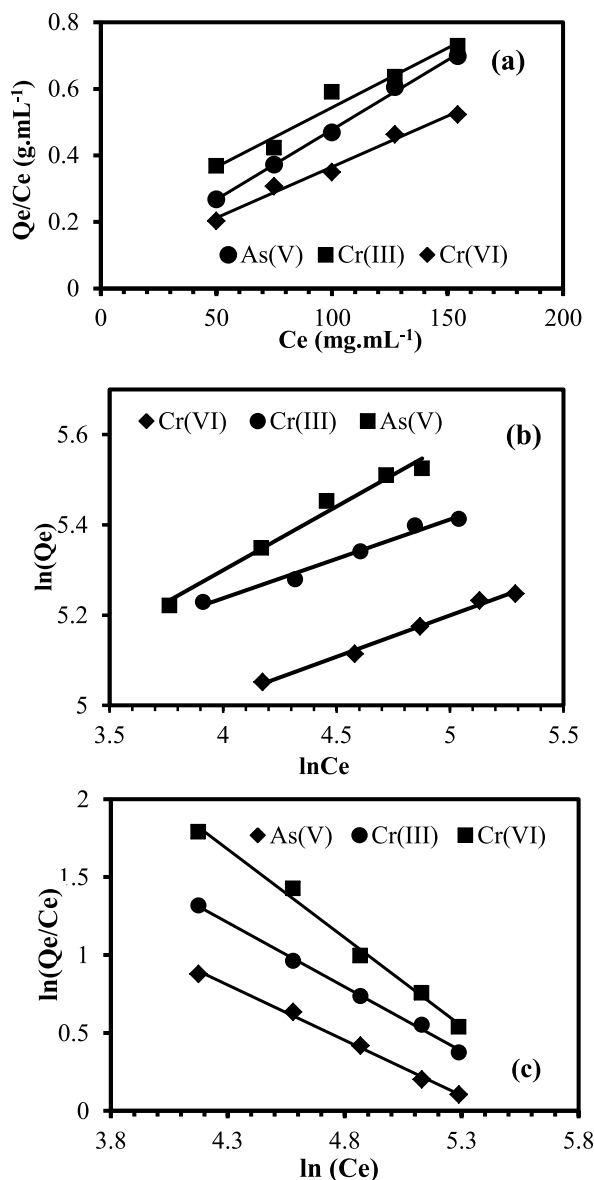

Fig. 4. Varification of Lamgmuir model via adsorption of pollutants on m-(HASG) (a). (b). Varification of Fruendlich model via adsorption of pollutants on m-(HASG), and varification of modified Fruendlich model via adsorption of pollutants on m-(HASG) (c).

Langmuir isotherm varifies the adsorptive competition on homogeneously exposed surface of m-(HASG). The physical constants, and respective R^2 values are represented in Table 2.

The non-homogeneity of surface may net be unnoticed due to dissimilarity DS crosslinking degree. Thus, adsorption on m-(HASG), was varified via Fruendlich model (Equation (4)). In which, Q_E gives adsorbate equilibrium amount, C_E is the final adsorbate concentration in solution, and K_f and n the constants associated with adsorption. Fig. 4b was constructed to obtain K_f and n against the targeted pollutants.

The well-known Fruendlich equation consider the different adsorption vacancies, and therefore remarkably high R^2 wa relevant physical constants were achieved (Table 2).

Further, modified fruendlich model parameters such as, K_{MF} (adsorption constant) and n_{MF} (adsorption intensity, dimensionless) were obtained the data points of plot between ln (Q_E/C_E) versus lnQ_E. The agreeable Fruendlich equation fit is shown from the plot in Fig. 4c.

4. Comparative survey of various adsorption isotherms

Adsorption models for example, Langmuir, Fruendlich, and modified models were varified, and the calculated physical parameters compared (Table 2). In case of Lamgmuir model, the rate constant (K_L) values were comparatively lower in comparison to Fruendlich (K_F) and modified Freundlich model rate constants (K_{MF}). This may be due to the fact that Langmuir model considers mono layer adsorption only, in addition with surface homogeneity [35]. In line with this, the R^2 values from obtained from Fruendlich based plot were comparable with the values from Lamgmuir model. The R^2 values from modified Freundlich model were notable with the calculated values approaching one. In case of modified Freundlich model, the K_F values were comparable to K_{MF} of Freundlich isotherm, and therefore is known as modified Freundlich isotherm. This is of great importance to describe that m-(HASG) based adsorption is quicker process that furnish various adsorption isotherms during waste water treatment.

5. Conclusion

The detailed synthetic route for micro dimension HASG preparation followed by successful modification with ᴅ-amine for potential application in waste water treatment is represented. The IEP values at pH 10.30 for HASG, and pH 2.97 for m-(HASG), and three folds increase in the HDR of m-(HASG) in comparison to HASG were observed upon the chemical modification. Finally, m-(HASG) were used as adsorbent for the removal of toxic contaminants from aqueous solution. It can be described that 100% Cr(VI) was removed from its aqueous solution (in DI and RW samples) by 0.15 g m-(HASG) in 2 h.

The adsorption on m-(HASG) follows various adsorption models such as, Langmuir, Freundlich, and modified Freundlich isotherms. It was deduced that among all the prescribed isotherms, the modified Freundlich isotherm give out best reasonable fit for all pollutants showing R^2 values of 0.9962, 0.9926, and for the adsorptions of As(V), Cr(VI), respectively in comparison with Langmuir and Freundlich models manifesting relatively lower R^2 values. To complete, the remarkable real water tests suggests that the HASG with chemically modifiable forms are promising natural polymers with great potential in the removal of toxic metal ions for environmental remediation purpose.

Author contribution statement

Rasha Kamal: Conceived and designed the experiments; Performed the experiments; Analyzed and interpreted the data; Contributed reagents, materials, analysis tools or data; Wrote the paper.

Data availability statement

Data will be made available on request.

Ethical approval

I confirm that we have read and have abided by the statement of ethical standard for manuscripts submitted to the journal.

Declaration of competing interest

The authors declare that they have no known competing financial interests or personal relationships that could have appeared to influence the work reported in this paper

Appendix A. Supplementary data

Supplementary data to this article can be found online at https://doi.org/10.1016/j.heliyon.2023.e17197.

Table 2

Comparative details of physical constants calculated by plotting data points of Langmuir, Freundlich and modified Freundlich linear equations.

Pollutant	Langmuir expressions			Fruendlich expressions			Modified Freundlich expressions		
	K_L [L.g^{-1}]	q_m [mg.g^1]	R^2	K_F [L.g^{-1}]	n_F	R^2	K_{MF} [L.g^{-1}]	n_{MF}	R^2
Arsenic(V)	0.0390	219.21	0.9983	73.14	5.54	0.9901	73.34	5.34	0.99723
Cr(VI)	0.050	256.40	0.9848	92.71	5.74	0.9931	93.72	5.73	0.9926
Cr (III)	0.41	273.21	0.9727	64.75	3.54	0.9902	85.33	4.70	0.9861

References

[1] B. Yu, et al., pH-responsive gelatin polymer-coated silica-based mesoporous composites for the sustained-release of indomethacin, Heliyon 9 (2023), e13705.
[2] N.N. Rudi, et al., Evolution of adsorption process for manganese removal in water via agricultural waste adsorbents, Heliyon 6 (9) (2020), e05049.
[3] B. Ekka, et al., Removal of Cr (VI) by silica-titania core-shell nanocomposites: in vivo toxicity assessment of the adsorbent by Drosophila melanogaster, Ceram. Int. 47 (13) (2021) 19079–19089.
[4] L. Verma, J. Singh, Removal of As(III) and As(V) from aqueous solution using engineered biochar: batch and fixed-bed column study, Int. J. Environ. Sci. Technol. 20 (2) (2023) 1961–1980.
[5] S. Sattar, et al., Composition, impacts, and removal of liquid petroleum waste through bioremediation as an alternative clean-up technology: a review, Heliyon (2022), e11101.
[6] A.M. Nasir, et al., Adsorptive nanocomposite membranes for heavy metal remediation: recent progresses and challenges, Chemosphere 232 (2019) 96–112.
[7] S. Sahu, et al., Investigating the selectivity and interference behavior for detoxification of Cr (VI) using lanthanum phosphate polyaniline nanocomposite via adsorption-reduction mechanism, Chemosphere 278 (2021), 130507.
[8] Z. Tattibayeva, et al., Peculiarities of adsorption of Cr (VI) ions on the surface of Chlorella vulgaris ZBS1 algae cells, Heliyon 8 (9) (2022), e10468.
[9] Y. Gao, et al., Potential threat of heavy metals and PAHs in PM2. 5 in different urban functional areas of Beijing, Atmos. Res. 178 (2016) 6–16.
[10] A. Chaturbedi, et al., Adsorption of positively and negatively charged heavy metal ions from wastewater by heteroaggregates of biopolymer particles, Colloids Surf. A Physicochem. Eng. Asp. 602 (2020), 124789.
[11] J. Xie, et al., Simultaneous Removal of Arsenic and Antimony from Mining Wastewater, 2020, pp. 117–119.
[12] J.W. Hamilton, et al., Molecular basis for effects of carcinogenic heavy metals on inducible gene expression, Environ. Health Perspect. 106 (suppl 4) (1998) 1005–1015.
[13] R. Mascher, et al., Arsenate toxicity: effects on oxidative stress response molecules and enzymes in red clover plants, Plant Sci. 163 (5) (2002) 961–969.
[14] T. Kamiya, et al., Phosphate deficiency signaling pathway is a target of arsenate and phosphate transporter OsPT1 is involved in as accumulation in shoots of rice, Soil Sci. Plant Nutr. 59 (4) (2013) 580–590.
[15] T. Davydiuk, et al., Removal of Inorganic Arsenic from Water Using Metal Organic Frameworks, 2020, pp. 162–168.
[16] A. Khamwichit, W. Dechapanya, W. Dechapanya, Adsorption kinetics and isotherms of binary metal ion aqueous solution using untreated venus shell, Heliyon 8 (6) (2022), e09610.
[17] P. Souda, L. Sreejith, Magnetic hydrogel for better adsorption of heavy metals from aqueous solutions, J. Environ. Chem. Eng. 3 (3) (2015) 1882–1891.
[18] H.E. Tahir, et al., Quality and postharvest-shelf life of cold-stored strawberry fruit as affected by gum Arabic (Acacia Senegal) edible coating, J. Food Biochem. 42 (3) (2018), e12527.
[19] A.A. Adetokun, S. Uba, Z.N. Garba, Optimization of adsorption of metal ions from a ternary aqueous solution with activated carbon from Acacia senegal (L.) Willd pods using Central Composite Design, J. King Saud Univ. Sci. 31 (4) (2019) 1452–1462.
[20] I. El-Garawani, et al., The ameliorative role of Acacia senegal gum against the oxidative stress and genotoxicity induced by the radiographic contrast medium (ioxitalamate) in albino rats, Antioxidants 10 (2) (2021) 221.
[21] T.R. Bhardwaj, et al., Natural gums and modified natural gums as sustained-release carriers, Drug Dev. Ind. Pharm. 26 (10) (2000) 1025–1038.
[22] M.R. Unnithan, V. Vinod, T. Anirudhan, Synthesis, characterization, and application as a chromium (VI) adsorbent of amine-modified polyacrylamide-grafted coconut coir pith, Ind. Eng. Chem. Res. 43 (9) (2004) 2247–2255.
[23] S. Rathinavel, et al., Synthesis and fabrication of amine functionalized SBA-15 incorporated PVA/Curcumin nanofiber for skin wound healing application, Colloids Surf. A Physicochem. Eng. Asp. 637 (2022), 128185.
[24] M. Jegelka, B. Plietker, Dual catalysis: vinyl sulfones through Tandem iron-catalyzed allylic sulfonation amine-catalyzed isomerization, ChemCatChem 4 (3) (2012) 329–332.
[25] Vani, T.S. and K.K. Rao, Recent Innovations in Natural Gums Based Adsorbents for the Removal of Toxic Metal Ion from Wastewater.
[26] K. Vimala, et al., Controlled silver nanoparticles synthesis in semi-hydrogel networks of poly (acrylamide) and carbohydrates: a rational methodology for antibacterial application, Carbohydr. Polym. 75 (3) (2009) 463–471.
[27] G. Tafuro, et al., Evaluating natural alternatives to synthetic acrylic polymers: rheological and texture analyses of polymeric water dispersions, ACS Omega 5 (25) (2020) 15280–15289.
[28] R. Uc-Peraza, V. Delgado-Blas, Acute toxicity and risk assessment of three commercial detergents using the polychaete Capitella sp. C from Chetumal Bay, Quintana Roo, Mexico, Int. Aquat. Res. 7 (4) (2015) 251–261.
[29] L.-C. Dong, A.S. Hoffman, Synthesis and application of thermally reversible heterogels for drug delivery, J. Contr. Release 13 (1) (1990) 21–31.
[30] A.E. Aferni, et al., The confinement of PVP in AOT microemulsions: effect of water content and PVP concentration regime on electrical percolation phenomenon, J. Mol. Liq. 318 (2020), 114012.
[31] S. Summonte, et al., Thiolated polymeric hydrogels for biomedical application: cross-linking mechanisms, J. Contr. Release 330 (2021) 470–482.
[32] M. Tajabadi, M.E. Khosroshahi, S. Bonakdar, An efficient method of SPION synthesis coated with third generation PAMAM dendrimer, Colloids Surf. A Physicochem. Eng. Asp. 431 (2013) 18–26.
[33] O. Madkhali, G. Mekhail, S.D. Wettig, Modified gelatin nanoparticles for gene delivery, Int. J. Pharm. 554 (2019) 224–234.
[34] M. Ghaedi, G. Negintaji, F. Marahel, Solid phase extraction and removal of brilliant green dye on zinc oxide nanoparticles loaded on activated carbon: new kinetic model and thermodynamic evaluation, J. Ind. Eng. Chem. 20 (4) (2014) 1444–1452.
[35] A.S. Bhatt, et al., Adsorption of an anionic dye from aqueous medium by organoclays: equilibrium modeling, kinetic and thermodynamic exploration, RSC Adv. 2 (23) (2012) 8663–8671.